Dynamic Long Short-Term Memory Neural-Network-Based Indirect Remaining-Useful-Life Prognosis for Satellite Lithium-Ion Battery

Cunsong Wang [1], Ningyun Lu [1,*], Senlin Wang [2], Yuehua Cheng [3] and Bin Jiang [1]

[1] College of Automation Engineering, Nanjing University of Aeronautics and Astronautics,
    Nanjing 211106, China; wangcunsong@nuaa.edu.cn (C.W.); binjiang@nuaa.edu.cn (B.J.)
[2] Quanzhou Institute of Equipment Manufacturing Haixi Institutes, Chinese Academy of Science,
    Quanzhou 362200, China; senlin16888@fjirsm.ac.cn
[3] College of Astronautics, Nanjing University of Aeronautics and Astronautics, Nanjing 210016, China;
    chengyuehua@nuaa.edu.cn
* Correspondence: luningyun@nuaa.edu.cn; Tel.: +86-025-5283-2301 (ext. 3140)

check for updates

Abstract: On-line remaining-useful-life (RUL) prognosis is still a problem for satellite Lithium-ion (Li-ion) batteries. Meanwhile, capacity, widely used as a health indicator of a battery (HI), is inconvenient or even impossible to measure. Aiming at practical and precise prediction of the RUL of satellite Li-ion batteries, a dynamic long short-term memory (DLSTM) neural-network-based indirect RUL prognosis is proposed in this paper. Firstly, an indirect HI based on the Spearman correlation analysis method is extracted from the battery discharge voltages, and the relationship between the indirect HI indices and battery capacity is established using a polynomial fitting method. Then, by integrating the Adam method, L2 regularization method, and incremental learning, a DLSTM method is proposed and applied for Li-ion battery RUL prognosis. Finally, verification of the results on NASA #5 battery data sets demonstrates that the proposed method has better dynamic performance and higher accuracy than the three other popular methods.

1. Introduction

Rechargeable lithium-ion (Li-ion) battery are widely applied in various satellites, because of their high-energy density, light weight, good performance, long lifetime, etc. [1]. Li-ion batteries are designed to supply power during a satellite's launch phase, shadow phase, and high load phase. However, after long-term, repeated charges and discharges, the lifetime of the Li-ion battery will be gradually reduced due to some irreversible reactions [2]. Li-ion battery degradation could result in the failure of satellite power subsystems, and even in a catastrophic occurrence. Therefore, it is critical to improve the safety and reliability of Li-ion battery in satellite systems, with the aid of a prognostic and health management (PHM) approach.

Technologically, PHM aims at predicting the current health status and the remaining useful life (RUL) of a system [3]. Specifically, the RUL prognosis [4–6] is the key technology of PHM to analyze, guarantee, and improve system safety and reliability. In general, the existing RUL prognosis of Li-ion batteries can be classified into three major categories: (1) experience-based approaches [7], such as the physicochemical ageing model, the weighted Ah ageing model, and the event-oriented ageing model; (2) model-based approaches, such as the Kalman filter (KF) [8–10] and particle filter (PF) [11–15]; and (3) data-driven approaches. Data-driven approaches also contain three major technologies: (1) time-series technology, such as the auto regressive (AR) and auto

regressive moving-average (ARMA) models [16]; (2) machine-learning technology, such as artificial neural networks (ANN) [17–19], support vector machine (SVM), or [4] relevance vector machine (RVM) [20,21]; and (3) statistical technology such as the Bayesian method [22,23] and Gaussian process regression (GPR) [24].

Data-driven approaches are attracting more attention than the other two approaches, since they need neither long term accumulation of the related experience, nor accurate aging mechanism of battery degradation phenomenon. Instead, data-driven approaches only depend on historical data, and use data mining, pattern recognition, and machine-learning techniques to forecast the RUL of Li-ion battery. In existing data-driven approaches, most researchers directly adopt capacity or resistance as health indicators (HI) [16–24]. In real applications, it is hard to measure and monitor Li-ion battery capacity or resistance directly. Meanwhile, to realize on-line RUL prognosis, computationally-efficient data-driven approaches are preferable.

A dynamic long short-term memory (DLSTM) neural-network-based indirect RUL prognosis for satellite Li-ion battery is proposed in this paper. The main contributions of this paper can be summarized as follows:

- For measured discharge voltages, a novel polynomial-fitting-based HI is constructed to replace Li-ion capacity for Li-ion battery RUL prognosis.
- Considering on-line and multi-step prediction, a DLSTM with the Adam method, L2 regularization method, and incremental learning idea is proposed.

The structure of this article is as follows. Section 2 briefly analyzes Li-ion battery data and clarifies the problem. Then, the proposed HI extraction and DLSTM methods are described in Section 3. Verification results are presented and analyzed in Section 4. Finally, Section 5 gives the conclusions and discusses future work.

2. Data Analysis and Problem Statement

2.1. Li-Ion Battery Data Analysis

In this paper, the NASA dataset [25] is exploited. It contains four different Li-ion batteries (#5, #6, #7, and #18), and each Li-ion battery repeats three operations (charge, discharge, and impedance measurements) at room temperature (24 °C). The test conditions of the NASA battery are listed in Table 1.

Table 1. Test condition of NASA battery data set.

Battery No.	Constant Charge Current/A	Charge Cut-off Voltage/V	Discharge Current/A	Discharge Cut-off Voltage/V	Nominal Capacity/Ah
5	**1.5**	**4.2**	**2.0**	**2.7**	**2.0**
6	1.5	4.2	2.0	2.5	2.0
7	1.5	4.2	2.0	2.2	2.0
18	1.5	4.2	2.0	2.5	2.0

Figure 1 shows the #5 Li-ion charge and discharge process in one cycle. Obviously, the charge process consists of constant current (CC) mode and constant voltage (CV) mode. In the charge in CC mode, the current is kept at 1.5 A until the Li-ion battery voltage is increased to 4.2 V. In the charge CV mode, the voltage holds 4.2 V until the Li-ion battery current drops to 20 mA from 1.5 A. In the whole charge process, the battery terminal voltage, battery output current, battery temperature, measured current, and measured voltage are recorded. The discharge process belongs to the CC mode, and the current is 2 A until the Li-ion battery voltage drops to 2.7 V from 4.2 V. In the discharge process, the recorded variables (except battery capacity) are the same as those of the charge process. Meanwhile, NASA Ames utilizes the electrochemical impedance spectroscopy (EIS) method (frequency sweep from 0.1 Hz to 5 kHz) to measure impedance. In the impedance process, the sensor current, battery current,

and ratio of the above currents are recorded to calculate battery impedance, electrolyte resistance (Re), and charge transfer resistance (Rct). As time goes on, the repeated charge and discharge process results in accelerated degradation, and eventually, the end of the battery's service life (EOL).
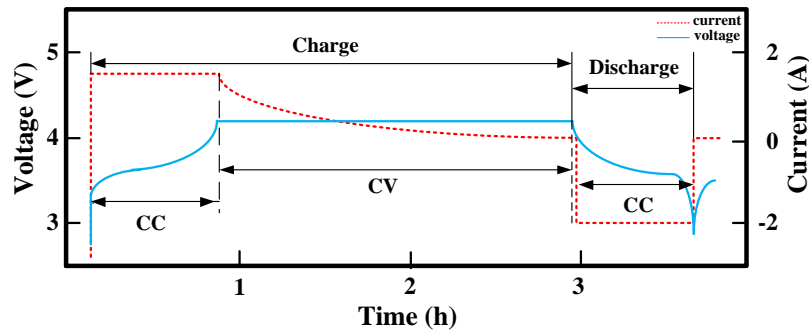
Figure 1. Charge and discharge process of Li-ion battery in one cycle [11].

2.2. Problem Statement

Typically, the EOL model of the Li-ion battery is closely related to that of a battery capacity [26]; the specific Li-ion battery remaining capacity model can be acquired in the literature [27]. This model gives all parameters (except some constant coefficients) by various experimental curve fittings. Despite knowledge of the complicated Li-ion mechanisms, the state of health (SOH) can be defined as:

$$SOH(\tau) = \frac{C(\tau)}{C(0)} \tag{1}$$

where $C(0)$ is the capacity value at the initial stage of Li-ion battery, and $C(\tau)$ is the capacity value at time τ (it is usually the index of cycle number).

Figure 2 gives the battery capacity changing curve according to the measured capacity of the discharge process. The curve clearly presents the degradation trend of a Li-ion battery. In the literature [28], Li-ion is regarded as being at EOL when its capacity drops to 70% (1.38 Ah) of its initial value. For satellite Li-ion batteries, it is inconvenient or even impossible to measure battery capacity values during in-orbit service. The main reason is that battery capacity measurements require the performance of a full charge and discharge cycle [29]. Hence, the problem is: how can we use basic measurements to construct a novel HI which can replace the capacity, and realize a dynamic RUL prognosis of Li-ion batteries used in satellites.
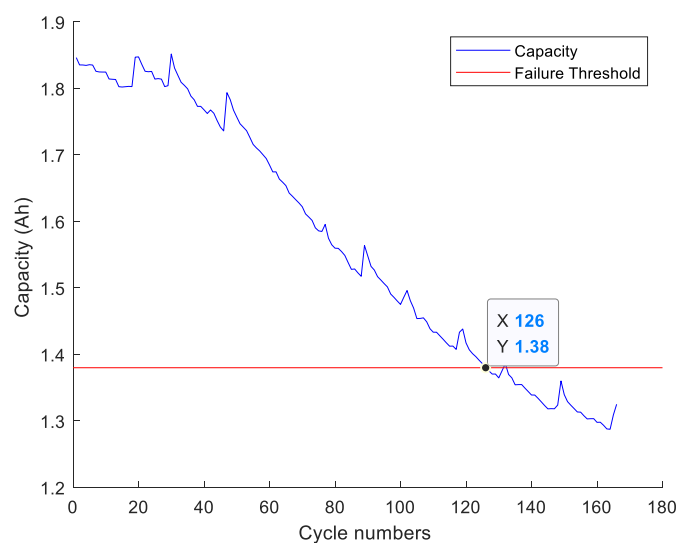
Figure 2. Capacity changing curve during the whole Li-ion battery life.

3. DLSTM Based Indirect RUL Prognosis

3.1. Polynomial Fitting Based HI

For Li-ion battery RUL prognosis, it is important to construct an indirect HI which shows the degradation phenomenon, because the battery capacity cannot be directly acquired on-line. In most real-life applications, the battery capacity can be estimated by one of a number of complex methods (electrochemical analysis, Ampere-hours, impedance, and other methods). These methods are time-consuming, and their accuracy is not satisfying. Therefore, using the charge current or discharge voltage to construct an indirect HI is more meaningful for online RUL prognosis.

It is widely known that a battery's life is closely related to its voltage. Similar to [30], we also adopt the time interval of equal discharge voltage difference (TIEDVD) as an indirect HI in each cycle. As shown in Figure 3, the Li-ion battery discharge time becomes shorter with each cycle. Due to the discrete monitoring time, the TIEDVD HI in the τth cycle can be defined as:

$$HI(\tau) = \max(T(\tau)) - \min(T(\tau)), \tau = 1, 2, ..., k \tag{2}$$

where $T(\tau)$ is the voltage measurement time aggregation of the τth cycle in the predefined discharge voltage range. The voltage range (Figure 3) contains Vmax (upper limit) and Vmin (lower limit). So, the HI series can be described as:

$$HI = \{HI(1), HI(2), ..., HI(k)\} \tag{3}$$
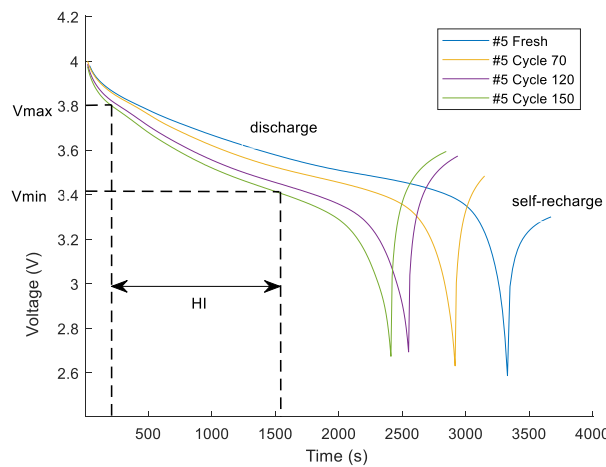
Figure 3. Discharge voltages at different cycle numbers and indirect HI extraction.

However, the literature [30] did not give the specific principle of discharge voltage range selection and the mapping relationship between the constructed HI and Li-ion battery capacity. Hence, in order to solve these problems, this paper utilizes the Spearman correlation coefficient method [31] to analyze and predefine the discharge voltage range. Spearman correlation analysis does not have specific data conditions, in contrast to two other correlation analysis methods (Person and Kendall). Then, the polynomial fitting method is used to analyze the correlation character [32] and establish the mapping relationship. Finally, the indirect HI construction framework can be summarized as follows:

Step 1: Acquire and preprocess the voltage measurements in each discharge cycle;

Step 2: Predefine the Vmax and Vmin, then use Equation (2) to calculate the HI of each cycle, and gain the HI series, as shown in Equation (3);

Step 3: Utilize Spearman method to calculate and analyze the correlation coefficient between the HI series and the Li-ion battery capacity series. If the correlation coefficient meets the demand, perform the next step. Otherwise, repeat Steps 2 and 3;

Step 4: Use the polynomial fitting method to build the mapping relationship between the HI and the Li-ion battery capacity.

3.2. DLSTM for RUL Prognosis

In this section, the LSTM [33] is introduced for Li-ion battery RUL prognosis. Compared with the recurrent neural network (RNN), the LSTM adds a memory cell structure which can solve the vanishing gradient problem and the exploding gradient problem. The LSTM is more suitable for time series prediction.

The basic LSTM architecture predictor is shown in Figure 4. Here, x_t is the input at the current time step, h_{t-1} stands for the output at the previous time step, and C_{t-1} is the cell memory at the previous time step; h_t stands for the output at the current time step, and C_t is the cell memory at the current time step. The red line (Figure 4) can maintain information transfer and not change the information through the whole cell state, which is the key to LSTM. The LSTM mainly contains a forget gate, input gate, input node, and output gate.
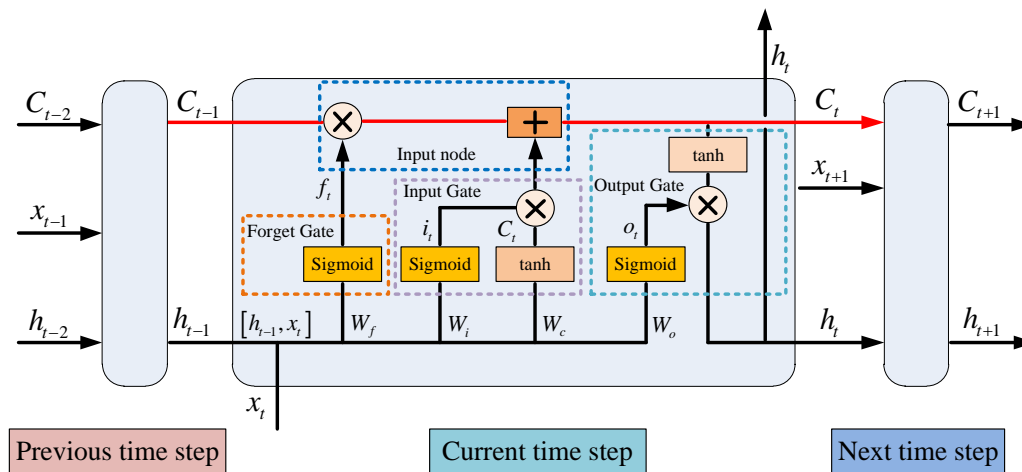
Figure 4. Basic LSTM architecture.

The forget gate is important; it can decide which information is discarded. For Li-ion battery RUL prognosis, the forget gate can discard some previous redundant information which does not influence the prediction result of next time step. The input gate and input node can determine which new information is stored. The output can realize the information output. Therefore, according to Figure 4, the essential formulas of LSTM are expressed as follows:

$$f_t = \sigma(W_f \cdot [h_{t-1}, x_t] + b_f) \tag{4}$$

$$i_t = \sigma(W_i \cdot [h_{t-1}, x_t] + b_i) \tag{5}$$

$$\widetilde{C}_t = \tanh(W_C \cdot [h_{t-1}, x_t] + b_C) \tag{6}$$

$$C_t = f_t * C_{t-1} + i_t * \widetilde{C}_t \tag{7}$$

$$o_t = \sigma(W_o \cdot [h_{t-1}, x_t] + b_o) \tag{8}$$

$$h_t = o_t * \tanh(C_t) \tag{9}$$

where σ is the sigmoid function; W_f, W_i, W_C and W_o are weight matrices; b_f, b_i, b_C and b_o are bias vectors.

When the LSTM is applied for Li-ion battery RUL prognosis, there are three problems. First, the traditional gradient descent methods, such as stochastic gradient descent (SGD), mini batch gradient descent, and RMSprop, cannot guarantee rapid convergence. They are also not suitable for on-line

RUL prognosis. The second problem is the overfitting phenomenon. The last problem is dynamic prediction with high accuracy.

In order to solve these problems associated with the deep learning in LSTM, this paper contributes three possible solutions. (1) Based on the resilient back-propagation algorithm [34] (Appendix A), this paper adopts the adaptive moment estimation (Adam) method [35] so that LSTM can have rapid convergence. The Adam method can avoid learning-rate loss, slow convergence, and significant change of loss function. The literature [35] has demonstrated that the Adam method can be applied for practical deep-learning problems, using large models and datasets. Therefore, we do not repeat it in this paper. (2) The L2 regularization method [36] is utilized to avoid overfitting. (3) Combining the incremental learning idea with the advantage of the forget gate, a dynamic long short-term memory neural network (DLSTM) is developed. The major steps of DLSTM for RUL prognosis can be summarized as follows:

Step 1: Partition the training data and test data according to the acquired indirect HI time series in Section 3.1. The training data is used as the input of DLSTM;

Step 2: In the process of forward propagation, calculate the six intermediate parameters f_t, i_t, $\widetilde{C}_t$, C_t, o_t and h_t according to Equations (4)–(9);

Step 3: In the process of resilient back-propagation (as shown in Equations (A1)–(A7)), add the L2 regularization method to avoid overfitting, and utilize the Adam method to update the matrices W_f, W_i, W_C, and W_o, and the bias vectors b_f, b_i, b_C, and b_o;

Step 4: Output the next five prediction values;

Step 5: Use the acquired mapping relationship to transfer the prediction values to battery capacity;

Step 6: If the predicted values exceed the failure threshold, perform the next step. If not, add five new prediction values to the training data, update the neural network structure dynamically, and repeat Steps 2–6;

Step 7: Output the predicted RUL of Li-ion battery.

3.3. Evaluation Criterion

In this paper, root mean square error (*RMSE*), mean absolute error (*MAE*), and RUL predicted error (*RUL$_{error}$*) are used to evaluate the prediction performance:

$$RMSE = \sqrt{\frac{1}{t} \sum_{i=1}^{t} (y_i - f(x_i))^2} \tag{10}$$

$$MAE = \frac{1}{t} \sum_{i=1}^{t} \|y_i - f(x_i)\| \tag{11}$$

$$RUL_{error} = RUL_{predict} - RUL_{true} \tag{12}$$

where y_i is the real value and $f(x_i)$ is the predicted value; $RUL_{predict}$ is the predicted RUL, and RUL_{true} is the true RUL.

4. Verification

4.1. Indirect HI Construction

In this section, the #5 satellite Li-ion battery (as described in Section 2.1) is used and handled to verify the proposed method of this paper.

Firstly according to Steps 1–3 in Section 3.1, the upper and lower limit voltages are set 3.8 V and 3.41 V respectively. Figure 5a,b gives the Li-ion battery capacity and indirect HI series curves. From the two figures, it is shown that the constructed indirect HI is very similar to Li-ion battery capacity, and the Spearman correlation coefficient between indirect HI series and Li-ion battery capacity series is equal to 0.9991. The result of Figure 5c also verifies the higher correlation. Finally, the mapping relationship between indirect HI and Li-ion battery capacity is obtained by the polynomial fitting

method. The specific mapping relationship can be expressed as a linear function; the parameters are, respectively, 0.0005 and 0.7193. According to the two parameters, the transfer result of indirect HI can be seen in Figure 5d.
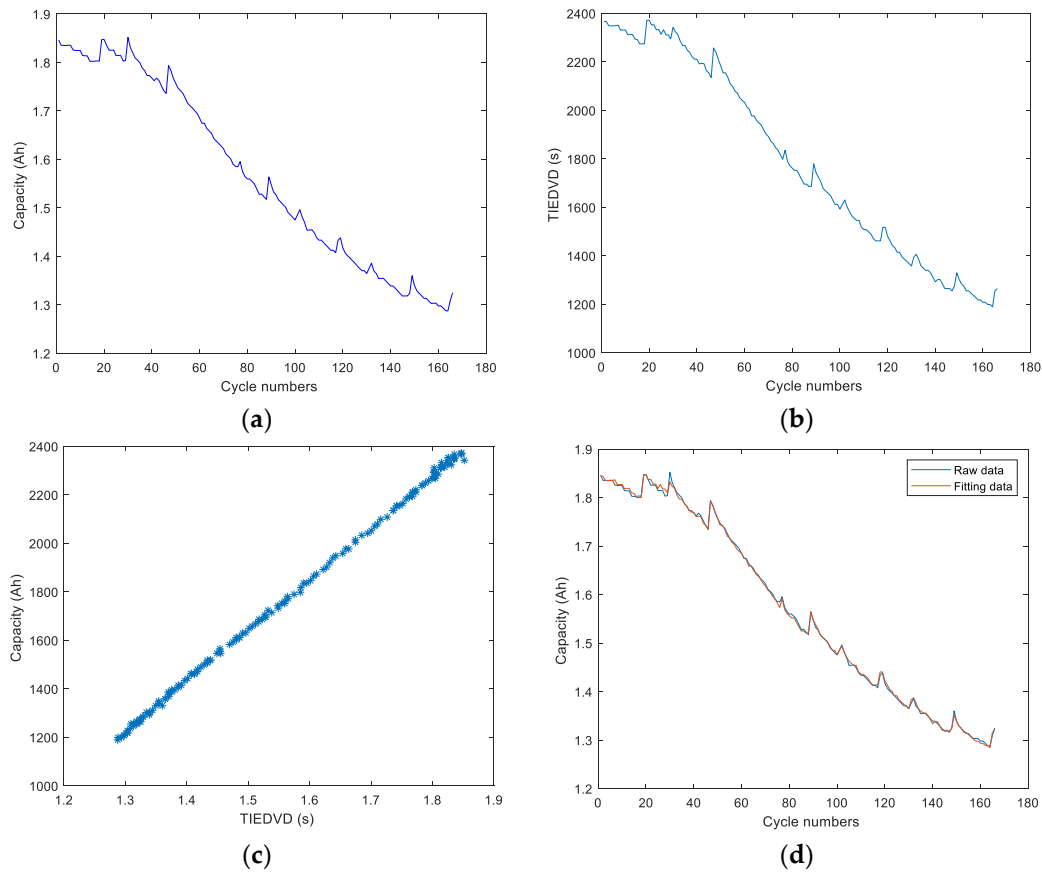
Figure 5. Indirect HI construction process: (**a**) capacity curve; (**b**) indirect HI curve; (**c**) correlation curve between indirect HI series and Li-ion battery capacity series; (**d**) mapping construction using polynomial fitting.

Therefore, the constructed indirect HI can replace Li-ion battery capacity for on-line RUL prognosis.

4.2. Li-Ion Battery RUL Prognosis

In this section, the constructed indirect HI series is divided into two parts: the 1 to 81 series data is training data; the remaining data is used as testing data.

Firstly, the neuron, the factor for dropping the learning rate, and the factor for L2 regularization (three major parameters of DLSTM) are set as 200, 0.3, and 0.1 respectively. Then, the proposed DLSTM, LSTM, ANN, and ARMA are used to predict the indirect HI series respectively. Finally, the prediction results of four methods are transferred to Li-ion battery capacity using the mapping relationship (in Section 4.1), and the RUL is calculated according to the failure threshold (described in Section 2.2).

Figure 6a–d show the RUL prognosis processes of four methods; the prediction performance comparison of four methods is listed in Table 1. Comparing Figure 6a,b, the proposed DLSTM has better dynamic performance than LSTM, and the error of RUL is very small. From Figure 6a–d and Table 2, it can be seen that the *RMSE, MAE,* and RUL_{error} of DLSTM are better than LSTM, ANN and ARMA.
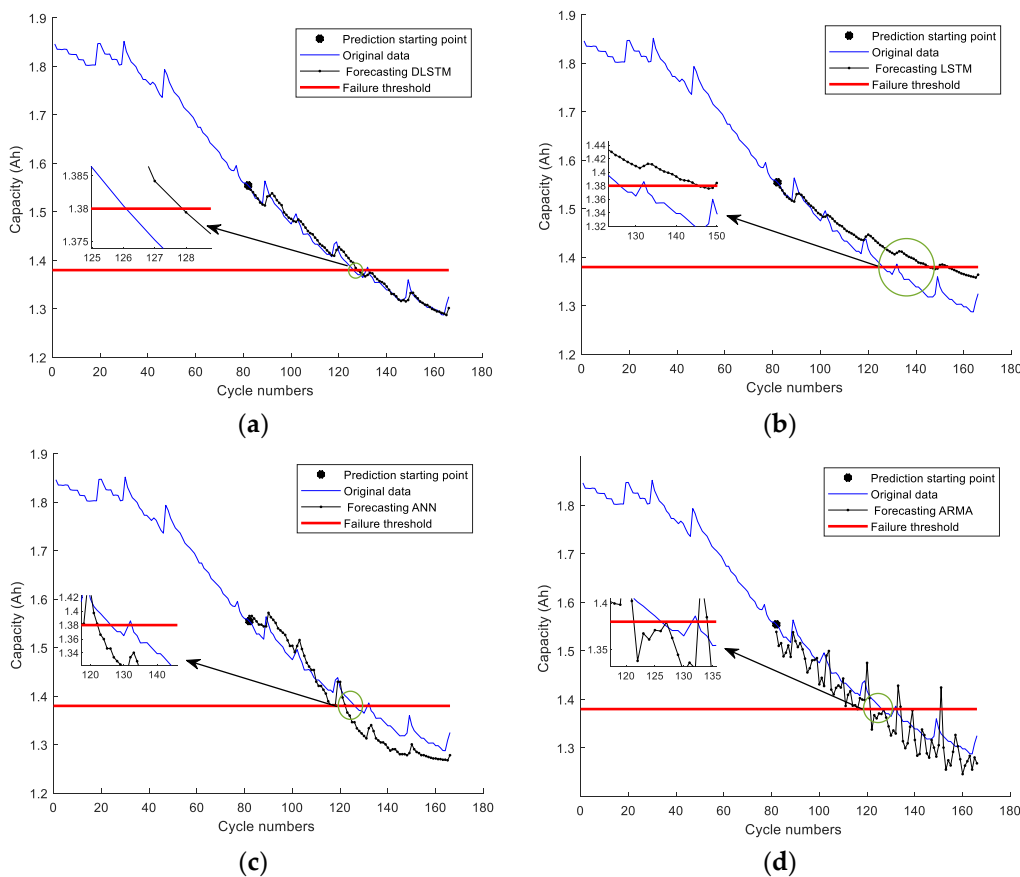
Figure 6. Comparison of four different methods for satellite Li-ion battery RUL prognosis: (**a**) DLSTM for RUL prognosis; (**b**) LSTM for RUL prognostic; (**c**) ANN for RUL prognosis; (**d**) ARMA for RUL prognosis.

Table 2. Prediction performance comparison of four methods.

Methods	*RMSE*	*MAE*	*RUL_{error}*
DLSTM	0.0119	0.0087	2
LSTM	0.0413	0.0348	20
ANN	0.0334	0.0303	−4
ARMA	0.0356	0.0302	−5

To summarize, the proposed DLSTM method based on indirect HI has good dynamic performance, and is more suitable for satellite Li-ion battery long-term RUL prognosis.

5. Conclusions

Considering the unmeasured satellite Li-ion battery capacity and dynamic demand of RUL prognosis, a DLSTM-based, indirect RUL prognosis method is provided in this paper. This method can extract an indirect HI which can replace battery capacity and realize Li-ion battery on-line RUL prognosis. The verification results on NASA #5 battery data sets demonstrate the feasibility and effectiveness of the proposed method.

However, the operation conditions and environment are constant in this paper. The Li-ion battery RUL, based on different operations and environments, will be considered in future research. Furthermore, the management of uncertainties is also important for the PHM of Li-ion battery. Its main purpose is to analyze the influence of various uncertainties, and provide a confidence coefficient for predictions. In future, Bayesian theory, particle filter, or other uncertainty technologies will be considered and added to realize the management of uncertainties of Li-ion batteries.

Appendix A.

Here, we give the brief resilient back-propagation calculation process of LSTM. Firstly, we define:

$$W \cdot s_t = \begin{bmatrix} W_f \\ W_i \\ W_C \\ W_o \end{bmatrix} \cdot s_t = \begin{bmatrix} W_f h W_f x b_f \\ W_i h W_i x b_i \\ W_C h W_C x b_C \\ W_o h W_o x b_o \end{bmatrix} \cdot \begin{bmatrix} h_{t-1} \\ x_t \\ 1 \end{bmatrix} \tag{A1}$$

Then, we assume $\frac{\partial E^t}{\partial h^t} = \delta h^t$, where E^t is the error at time t. Next, we will calculate the gradient of LSTM (orderly solve as shown in Figure A1). δo^t and δo^t are acquired by Equation (A2); δf_t, δi_t, $\delta \widetilde{C}_t$ and δC^{t-1} acquired by Equation (A3); δW_f, δW_i, δW_C and δW_o are acquired by Equations (A4) and (A5). Therefore, the total gradient can be summarized as Equation (A6). Finally, the matrix W can be updated as Equation (A7).

$$\begin{aligned} \delta o^t = \frac{\partial E^t}{\partial o^t} = \delta h^t \odot \tanh(C^t) \\ \delta C^t = \frac{\partial E^t}{\partial C^t} = \delta h_i^t \odot o^t \odot [1 - \tanh^2(C^t)] \end{aligned} \tag{A2}$$

$$\begin{aligned} \delta f^t = \frac{\partial E^t}{\partial f^t} = \delta C^t \odot C^{t-1} \\ \delta i^t = \frac{\partial E^t}{\partial i^t} = \delta C^t \odot \widetilde{C}^t \\ \delta C^{t-1} = \frac{\partial E^t}{\partial C^{t-1}} = \delta C^t \odot f^t \\ \delta \widetilde{C}^t = \frac{\partial E^t}{\partial \widetilde{C}_i^t} = \delta C^t \odot i^t \end{aligned} \tag{A3}$$

$$\begin{aligned} \frac{\partial E^t}{\partial W_f} = [\delta f^t \odot f^t \odot (1 - f^t)] \otimes (s^t)^T \\ \frac{\partial E^t}{\partial W_i} = [\delta i^t \odot i^t \odot (1 - i^t)] \otimes (s^t)^T \\ \frac{\partial E^t}{\partial W_o} = [\delta o^t \odot o^t \odot (1 - o^t)] \otimes (s^t)^T \\ \frac{\partial E^t}{\partial W_C} = [\delta \widetilde{C}^t \odot (1 - (\widetilde{C}^t)^2)] \otimes (s^t)^T \end{aligned} \tag{A4}$$

$$\frac{\partial E^t}{\partial W} = \begin{bmatrix} \delta f^t \odot f^t \odot (1 - f^t) \\ \delta i^t \odot i^t \odot (1 - i^t) \\ \delta o^t \odot o^t \odot (1 - o^t) \\ \delta \widetilde{C}^t \odot (1 - (\widetilde{C}^t)^2) \end{bmatrix} \otimes (s^t)^T \tag{A5}$$

$$\frac{\partial E}{\partial W} = \sum_{t=0}^{T} \frac{\partial E^t}{\partial W} \tag{A6}$$

$$W = W - \eta \frac{\partial E}{\partial W} \tag{A7}$$
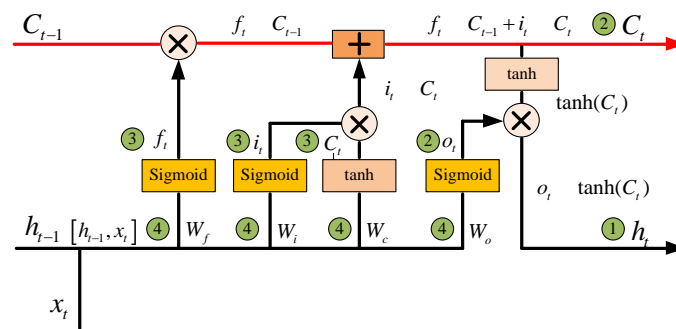
Figure A1. Back-propagation errors of four different stages.

References

1. Song, Y.; Liu, D.; Yang, C.; Peng, Y. Data-driven hybrid remaining useful life estimation approach for spacecraft lithium-ion battery. *Microelectron. Reliab.* **2017**, *75*, 142–153. [CrossRef]
2. Vetter, J.; Novák, P.; Wagner, M.R.; Veit, C.; Möller, K.C. Ageing mechanisms in lithium-ion batteries. *J. Power Sources* **2005**, *147*, 269–281. [CrossRef]
3. Javed, K.; Gouriveau, R.; Zerhouni, N. State of the art and taxonomy of prognostics approaches, trends of prognostics applications and open issues towards maturity at different technology readiness levels. *Mech. Syst. Signal Process.* **2017**, *94*, 214–236. [CrossRef]
4. Patil, M.A.; Tagade, P.; Hariharan, K.S.; Kolake, S.M.; Song, T.; Yeo, T.; Doo, S. A novel multistage support vector machine based approach for Li-ion battery remaining useful life estimation. *Appl. Energy* **2015**, *159*, 285–297. [CrossRef]
5. Zhou, H.W.; Huang, J.Q.; Lu, F. Reduced kernel recursive least squares algorithm for aero-engine degradation prediction. *Mech. Syst. Signal Process.* **2017**, *95*, 446–467. [CrossRef]
6. Wang, X.; Jiang, B.; Lu, N.; Cocquempot, V. Accurate prediction of RUL under uncertainty conditions: Application to the traction system of a high-speed train. In Proceedings of the 10th IFAC Symposium on Fault Detection, Supervision and Safety for Technical Processes, IFAC Safe Process 2018, Warsaw, Poland, 29–31 August 2018.
7. Sauer, D.U.; Wenzl, H. Comparison of different approaches for lifetime prediction of electrochemical systems—Using lead-acid batteries as example. *J. Power Sources* **2008**, *176*, 534–546. [CrossRef]
8. Remmlinger, J.; Buchholz, M.; Soczka-Guth, T.; Dietmayer, K. On-board state-of-health monitoring of lithium-ion batteries using linear parameter-varying models. *J. Power Sources* **2013**, *239*, 689–695. [CrossRef]
9. Zheng, X.J.; Fang, H.J. An integrated unscented kalman filter and relevance vector regression approach for lithium-ion battery remaining useful life and short-term capacity prediction. *Reliab. Eng. Syst. Saf.* **2015**, *144*, 74–82. [CrossRef]
10. Plett, G.L. Extended Kalman filtering for battery management systems of LiPB-based HEV battery packs. *J. Power Sources* **2004**, *134*, 252–261. [CrossRef]
11. Wei, J.W.; Dong, G.Z.; Chen, Z.H. Remaining useful life prediction and state of health diagnosis for Lithium-Ion batteries using particle filter and support vector regression. *IEEE Trans. Ind. Electron.* **2018**, *65*, 5634–5643. [CrossRef]
12. Li, D.Z.; Wang, W.; Ismail, F. A mutated particle filter technique for system state estimation and battery life prediction. *IEEE Trans. Instrum. Meas.* **2014**, *63*, 2034–2043. [CrossRef]
13. Miao, Q.; Xie, L.; Cui, H.; Liang, W.; Pecht, M. Remaining useful life prediction of lithium-ion battery with unscented particle filter technique. *Microelectron. Reliab.* **2013**, *53*, 805–810. [CrossRef]
14. Liu, Z.; Sun, G.; Bu, S.; Han, J.; Tang, X.; Pecht, M. Particle learning framework for estimating the remaining useful life of Lithium-Ion batteries. *IEEE Trans. Instrum. Meas.* **2017**, *66*, 280–293. [CrossRef]
15. Su, X.; Wang, S.; Pecht, M.; Zhao, L.; Ye, Z. Interacting multiple model particle filter for prognostics of lithium-ion batteries. *Microelectron. Reliab.* **2017**, *70*, 59–69. [CrossRef]
16. Long, B.; Xian, W.; Jiang, L.; Liu, Z. An improved autoregressive model by particle swarm optimization for prognostics of lithium-ion batteries. *Microelectron. Reliab.* **2013**, *53*, 821–831. [CrossRef]

17. Liu, J.; Saxena, A.; Goebel, K.; Saha, B.; Wang, W. An adaptive recurrent neural network for remaining useful life prediction of Lithium-ion batteries. In Proceedings of the Annual Conference of the Prognostics and Health Management Society 2010 (PHM 2010), Portland, OR, USA, 13–16 October 2010.

18. Chaoui, H.; Ibe-Ekeocha, C.C.; Gualous, H. Aging prediction and state of charge estimation of a LiFePO$_4$ battery using input time-delayed neural networks. *Electr. Power Syst. Res.* **2017**, *146*, 189–197. [CrossRef]

19. Xia, B.; Cui, D.; Sun, Z.; Lao, Z.; Zhang, R.; Wang, W.; Sun, W.; Lai, Y.; Wang, M. State of charge estimation of lithium-ion batteries using optimized Levenberg-Marquardt wavelet neural network. *Energy* **2018**, *153*, 694–705. [CrossRef]

20. Liu, D.; Zhou, J.; Pan, D.; Peng, Y.; Peng, X. Lithium-ion battery remaining useful life estimation with an optimized relevance vector machine algorithm with incremental learning. *Measurement* **2015**, *63*, 143–151. [CrossRef]

21. Zhou, Y.; Huang, M.; Chen, Y.; Tao, Y. A novel health indicator for on-line lithium-ion batteries remaining useful life prediction. *J. Power Sources* **2016**, *321*, 1–10. [CrossRef]

22. Ng, S.S.Y.; Xing, Y.; Tsui, K.L. A naive Bayes model for robust remaining useful life prediction of lithium-ion battery. *Appl. Energy* **2014**, *118*, 114–123. [CrossRef]

23. Cheng, Y.; Lu, C.; Li, T.; Tao, L. Residual lifetime prediction for lithium-ion battery based on functional principal component analysis and Bayesian approach. *Energy* **2015**, *90*, 1983–1993. [CrossRef]

24. Yang, D.; Zhang, X.; Pan, R.; Wang, Y.; Chen, Z. A novel Gaussian process regression model for state-of-health estimation of lithium-ion battery using charging curve. *J. Power Sources* **2018**, *384*, 387–395. [CrossRef]

25. Saha, B.; Goebel, K. *Battery Data Set, NASA Ames Prognostics Data Repository*; NASA Ames: Moffett Field, CA, USA, 2007. Available online: https://ti.arc.nasa.gov/tech/dash/groups/pcoe/prognostic-data-repository/ (accessed on 5 March 2018).

26. Lu, L.; Han, X.; Li, J.; Hua, J.; Ouyang, M. A review on the key issues for lithium-ion battery management in electric vehicles. *J. Power Sources* **2013**, *226*, 272–288. [CrossRef]

27. Rong, P.; Pedram, M. An analytical model for predicting the remaining battery capacity of Lithium-Ion batteries. *IEEE Trans. Very Large Scale Integr. Syst.* **2006**, *14*, 441–451. [CrossRef]

28. Goebel, K.; Saha, B.; Saxena, A.; Celaya, J.R. Prognostics in battery health management. *IEEE Instrum. Meas. Mag.* **2008**, *11*, 33–40. [CrossRef]

29. Tang, X.; Zou, C.; Yao, K.; Chen, G.; Liu, B.; He, Z.; Gao, F. A fast estimation algorithm for lithium-ion battery state of health. *J. Power Sources* **2018**, *396*, 453–458. [CrossRef]

30. Liu, D.; Wang, H.; Peng, Y.; Xie, W.; Liao, H. Satellite Lithium-Ion battery remaining cycle life prediction with novel indirect health indicator extraction. *Energies* **2013**, *6*, 3654–3668. [CrossRef]

31. Gautheir, T.D. Detecting trends using spearman's rank correlation coefficient. *Environ. Forensics* **2001**, *2*, 359–362. [CrossRef]

32. Elaheh, A.; Mehmed, K. SOM-based partial labeling of imbalanced data stream. *Neurocomputing* **2017**, *262*, 120–133.

33. Gers, F.A.; Schmidhuber, J.; Cummins, F. Learning to forget: Continual prediction with LSTM. In Proceedings of the 9th International Conference on Artificial Neural Networks, (ICANN'99), Edinburgh, UK, 7–10 September 1999; pp. 850–855.

34. Riedmiller, M.; Braun, H. A direct adaptive method for faster backpropagation learning: The RPROP algorithm. *Chem. Prod. Process Model.* **1993**, *6*, 586–591.

35. Kingma, D.; Ba, J.L. Adam: A method for stochastic optimization. *arXiv* **2014**, arXiv:1412.6980.

36. Tikhonov, A.N. On the stability of inverse problems. *Dolklady Akademii Nauk SSSR* **1943**, *39*, 195–198.